DOI: 10.1002/ejic.201000790

Enhanced Photostability from CdSe(S)/ZnO Core/Shell Quantum Dots and Their Use in Biolabeling

Fadi Aldeek,[a,b] Christian Mustin,[c] Lavinia Balan,[d] Ghouti Medjahdi,[e] Thibault Roques-Carmes,[b] Philippe Arnoux,[b] and Raphaël Schneider*[b]

Keywords: Quantum dots / Synthesis design / Fluorescence

We report on the preparation and on the photophysical and structural characterization of alloyed CdSe(S) nanocrystals, which are covered by a ZnO shell. CdSe(S) QDs were prepared by reaction of $CdCl_2$ with NaHSe in the presence of 3-mercaptopropionic acid (MPA) under hydrothermal conditions. The incorporation of sulfur arises from the surface-mediated MPA hydrolysis on the growing QD surface. Water-dispersible CdSe(S) QDs were successfully capped with a ZnO shell obtained by basic hydrolysis of $Zn(OAc)_2$. The experimental results from transmission electron microscopy (TEM) imaging and powder X-ray diffractometry (XRD) analyses indicate that the core/shell CdSe(S)/ZnO QDs have a very small diameter (ca. 2.8 nm) and exhibit a face-centered cubic crystal structure. Our results show that core/shell CdSe(S)/ZnO QDs have a higher photostability than CdSe(S) cores. CdSe(S)/ZnO QDs have potential applications as fluorescent biological labels and were successfully used for imaging *Schewanella oneidensis* bacterial biofilms.

Introduction

Because of their unique size-dependent electrical and optical properties,[1] II–VI semiconductor quantum dots (QDs) have attracted great attention in recent years for their potential applications in biological labeling[2,3] and optoelectronic devices such as light-emitting diodes and photovoltaic cells.[4–9] QDs present many advantages relative to organic fluorophores such as high photoluminescence (PL) quantum yield, tunable emission wavelength, multiplexing capabilities, and high photoresistance. Among all the applications of QDs, biological labeling is currently of great interest. The prerequisite for the development of QD-based bioimaging systems is to gain access to water-dispersible and photostable nanocrystals.

The organometallic synthesis of QDs, the injection of reagents into a coordinating solvent such as tri-*n*-octylphosphane oxide (TOPO) at high temperature (200–400 °C), is an effective route to the preparation of high-quality QDs.[10] The nanocrystals thus prepared are, however, only soluble in nonpolar organic solvents, unless their surfaces are further modified with either thioacids or thioamines or that hydrophobic QDs are wrapped into micelles or polymers. The aqueous synthetic approach is an alternative strategy for the direct preparation of water-dispersed QDs. In addition, this method is cheaper, simpler, and less toxic. In recent years, methods for preparing CdSe or CdTe QDs in water solution either by heating at 100 °C, by the hydrothermal method or by microwave-assisted synthesis have significantly improved.[11–17]

The surface passivation by growing an inorganic shell of a wider band gap semiconductor on II–VI QDs is an important parameter to improve the PL quantum yield and the photo/thermal stability of these nanocrystals by decreasing nonradiative recombination.[18,19] Indeed, if the band gap of the core is enclosed by that of the shell, then the wave functions of electrons and holes are confined within the core region, which thus reduces the probability of nonradiative decay into surface states and trap sites.[20,21] Various II–VI semiconductors have been investigated as shell material for CdSe QDs to improve the PL quantum yields and the chemical stability. However, core/shell CdSe/ZnS[22,23] or CdSe/CdS[24,25] or core/shell/shell or multishell CdSe/CdS/ZnS[26–28] QDs are generally prepared by the successive ion layer adhesion and reaction (SILAR) technique.

In comparison with organometallic synthesis, little attention has been paid to the introduction of an inorganic shell on CdSe core QDs in aqueous solution until now. In this paper, we describe the epitaxial overcoat of a ZnO shell on the outerlayer of alloyed CdSe(S) nanocrystals to obtain CdSe(S)/ZnO core/shell heterostructures. The additional ZnO shell, with a substantially wide bang gap, serves as a

[a] LCPME, UMR 7564, Nancy University, CNRS, 405, rue de Vandoeuvre, 54506 Villers-lès-Nancy, France
[b] LRGP, UPR 3349, Nancy University, CNRS, 1 rue Grandville, 54001 Nancy, France
E-mail: raphael.schneider@ensic.inpl-nancy.fr
[c] LIMOS, UMR 7137, Nancy-University, CNRS, Faculté des Sciences, B. P. 239, 54506 Vandoeuvre-les-Nancy, France
[d] IS2M, LRC 7228, 15 rue Jean Starcky, 68093 Mulhouse, France
[e] IJL, Nancy-University, CNRS, B. P. 70239, 54506 Vandoeuvre-lès-Nancy, France
Supporting information for this article is available on the WWW under http://dx.doi.org/10.1002/ejic.201000790.

 WILEY ONLINE LIBRARY © 2011 Wiley-VCH Verlag GmbH & Co. KGaA, Weinheim

type I heterojunction (the band offsets among CdSe, CdS, and ZnO are shown in Figure 1). Our experimental results show that the quantum efficiency and the photostability were improved by adding the ZnO shell because of better surface passivation of the CdSe(S) cores. Core/shell CdSe(S)/ZnO QDs nanocrystals were successfully used as fluorescence probes for the labeling of bacterial biofilms.

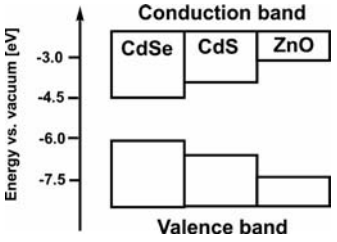

Figure 1. Energetic band positions of semiconductor material combinations used in this work.

Results and Discussion

Synthesis of MPA-Capped Core/Shell CdSe(S)/ZnO Nanocrystals

The CdSe core QDs were synthesized according to the following chemical reactions by using 3-mercaptopropionic acid (MPA) as stabilizer.

$$2Se + 4NaBH_4 + 7H_2O \rightarrow 2NaHSe + Na_2B_4O_7 + 14H_2$$

$$CdCl_2 + NaHSe + NaOH \rightarrow CdSe + 2NaCl + H_2O$$

We took advantage of an autoclave to obtain a high temperature (150 °C) and pressure to accelerate the growth of the CdSe nanocrystals. As reported for CdTe QDs,[29,30] during the heating phase, a part of the MPA ligand is hydrolyzed and serves as sulfur source to produce alloyed CdSe(S) QDs, which has a gradient of sulfur from the inside to the surface of the nanocrystals that depends on the competition between MPA decomposition and the rate of S^{2-} vs. Se^{2-} addition to a growing QD surface.

The CdSe(S)/ZnO core/shell QDs were prepared by the slow injection of a 0.01 M aqueous solution of $Zn(OAc)_2$ to the crude CdSe(S) QDs under atmospheric pressure and by further heating at reflux for 2 h. At basic pH [the pH value measured at the end of the hydrothermal synthesis of CdSe(S) QDs was found to be 10.9], $Zn(OAc)_2$ is first hydrolyzed and converted into its hydroxide $Zn(OH)_2$. Dehydration of $Zn(OH)_2$ produces ZnO clusters that grow at the surface of the CdSe(S) nanocrystals to form the ZnO shell (Figure 2).

Size, Shape, Crystal Structure, and Photoluminescence Properties of CdSe(S)/ZnO Nanocrystals

Figure 3 a shows the typical UV/Vis absorption and PL spectra of the CdSe(S) nanocrystals obtained by reaction of $CdCl_2$ with NaHSe in the presence of MPA under hydrothermal conditions (150 °C, 1 h). In comparison with the spectrum for the syntheses conducted under normal pressure at 100 °C,[14] the PL spectrum of the CdSe(S) cores does not show a shallow trap emission because of incomplete passivation. The luminescence of MPA-capped CdSe(S) QDs is dominated by near-band-edge luminescence at 511 nm (PL quantum yield of 13%). The Stokes shift is small (15 nm) and the full-width-at-half-maximum (fwhm) is narrow (56 nm). The average diameter of the CdSe(S) nanocrystals was calculated to be 2.2 nm by using the first exciton absorption peak of the UV/Vis absorption spectrum.[31] Figure 4a shows a typical TEM image of these nanocrystals. The CdSe(S) cores are close to spherical and their average diameter is 2.5 ± 0.5 nm.

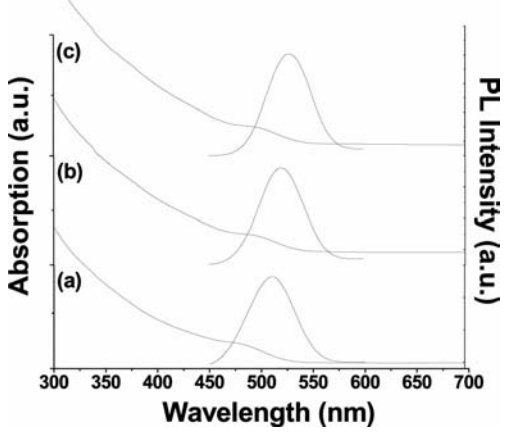

Figure 3. UV/Vis absorption and PL spectra of (a) core CdSe(S) QDs, (b) CdSe(S)/ZnO QDs (Zn/Cd = 0.2), and (c) CdSe(S)/ZnO QDs (Zn/Cd = 0.4).

After the addition of the ZnO shell under alkaline conditions, both absorption and PL spectra of the QDs shift to higher wavelengths. As shown in Figure 3b and c, the exci-

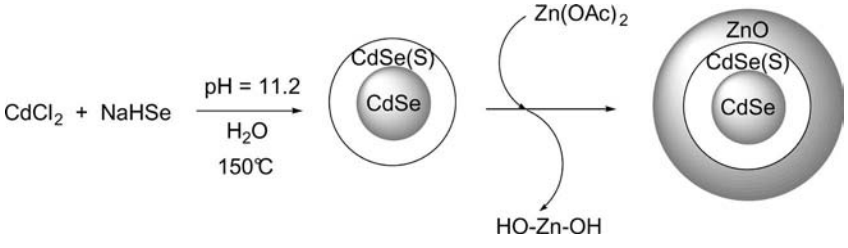

Figure 2. Schematic of the synthesis of water-soluble CdSe(S)/ZnO core/shell nanocrystals.

 © 2011 Wiley-VCH Verlag GmbH & Co. KGaA, Weinheim

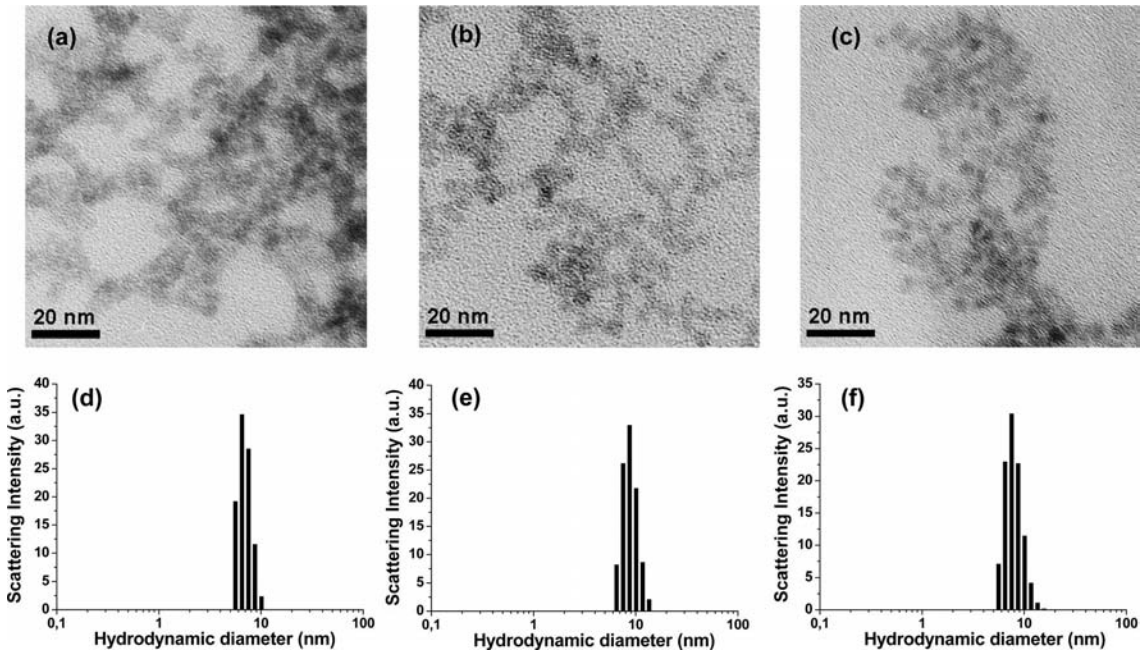

Figure 4. TEM images of (a) core CdSe(S) QDs, (b) CdSe(S)/ZnO QDs prepared with a Zn/Cd ratio of 0.2, (c) CdSe(S)/ZnO QDs prepared with a Zn/Cd ratio of 0.4. (d), (e), and (f), the corresponding hydrodynamic sizes measured by DLS.

ton peaks of the QD system shift to the red from 482 to 495 and 496 nm, respectively, for Zn/Cd ratios of 0.2 and 0.4. Meanwhile, the corresponding PL emission wavelengths shift from 511 to 522 and 527 nm, and the fwhms of the PL spectra decrease from 56 nm for core CdSe(S) QDs to 53 and 47 nm, respectively, for CdSe(S)/ZnO core/shell QDs prepared with Zn/Cd ratios of 0.2 and 0.4. Relative to the PL quantum yield of the core CdSe(S)@MPA crude solution (13%), that of the new core/shell QDs prepared with a Zn/Cd ratio of 0.2 is enhanced by about 1.5 times (20%), after heating at reflux for 2 h. With a Zn/Cd ratio of 0.4, the PL quantum yield reaches a plateau (24%). Similar observations were ascribed to the strain released through the formation of dislocations in the shell with increasing shell thickness, e.g. for core/shell CdSe/ZnS or core/shell/shell CdTe/CdS/ZnO QDs.[26,28,32] Further increasing the Zn/Cd ratio to 0.6 caused aggregation of QDs and confirmed the saturation effect observed during PL quantum yield measurements.

The TEM images of the core/shell CdSe(S)/ZnO QDs (Figure 4b and c) show that these nanocrystals have similar spherical morphologies to those of the CdSe(S) cores. The average diameters of the QDs prepared with Zn/Cd ratios of 0.2 and 0.4 were determined to be 2.8 ± 0.4 and 2.9 ± 0.7 nm, respectively; these values are close to those calculated from the absorption spectra and consistent with average diameters calculated by AFM (see Figure S1). Dynamic light-scattering (DLS) measurements indicate that the QDs are well dispersed in water and that their hydrodynamic diameters range from ca. 7.5 to 10 nm [the average hydrodynamic diameters determined for CdSe(S) cores and core/shell QDs prepared with Zn/Cd ratios of 0.2 and 0.4 are 7.7 ± 1.7, 9.1 ± 2.6, and 9.9 ± 3.5 nm, respectively] (Figure 4d–f). The hydrodynamic diameter is larger than the diameter of the inorganic core because of the solvation layer around the QDs in aqueous solution.

The crystal form of the CdSe(S) alloyed core was characterized with XRD patterns and the results are shown in Figure 5a. The broadness of the peaks is attributed to the

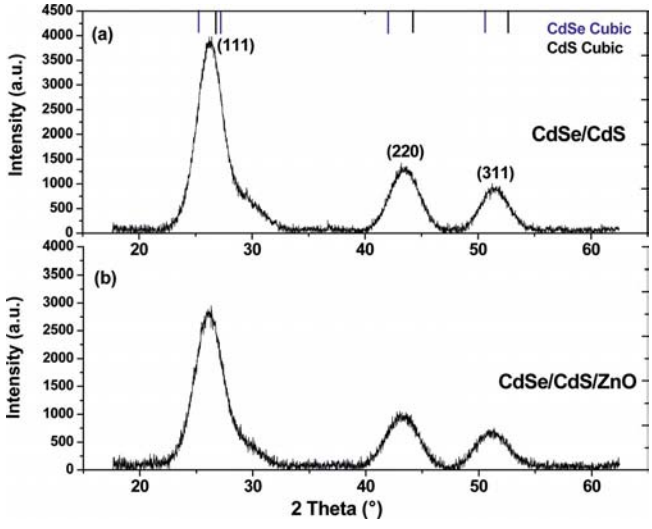

Figure 5. Powder XRD pattern of the CdSe(S) nanocrystals (a) before and (b) after introduction of the ZnO shell (QDs prepared with a Zn/Cd ratio of 0.4). The standard diffraction lines for zinc blende CdSe (above, blue) and zinc blende CdS (above, black) are also shown.

 © 2011 Wiley-VCH Verlag GmbH & Co. KGaA, Weinheim

small dimensions of the nanocrystals. The peaks at 2θ = 26.2, 43.4, and 51.4° correspond to the (111), (220), and (311) planes of the zinc blende phase of CdSe crystallizing in the $F\bar{4}3m$ space group as shown by the bars in the upper part of the JCPDS card, N° 19–0191. The crystallization of CdSe in the cubic phase was possible because of the low growth temperature (150 °C) employed for the synthesis of the CdSe nanocrystals and the absence of phosphanes in the reaction medium.[33] The XRD reflections deviate to larger angles between the values of the cubic CdSe and the cubic CdS phases, which gives evidence that the nanocrystals cores are CdSe(S) alloyed QDs. The size obtained from the XRD pattern (2.5 ± 1.0 nm, see Figure S2) agrees well with that estimated by TEM and absorption spectroscopy. For the core/shell QDs (Figure 4b), no peak shift is observed as a result of the thin shell thickness (≈0.5–1.0 nm) that does not contract the lattice of the CdSe(S) core.

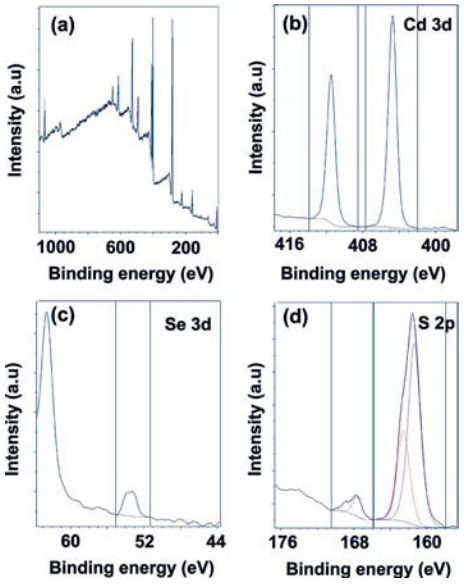

Figure 6. XPS spectra of CdSe(S) QDs. (a) XPS survey spectrum. Binding energy spectra of (b) Cd 3d, (c) Se 3d, and (d) S 2p.

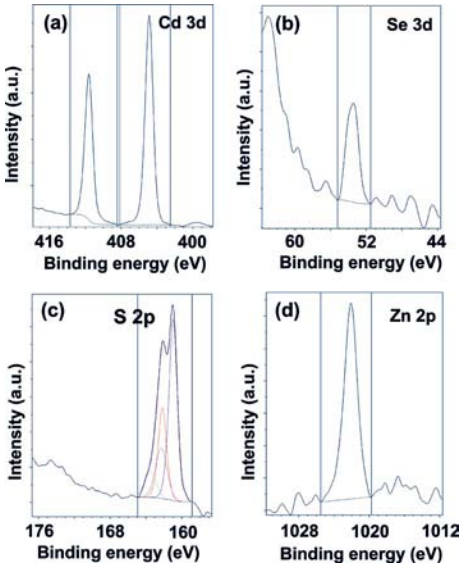

Figure 7. XPS spectra of core/shell CdSe(S)/ZnO QDs. Binding energy of (a) Cd 3d, (b) Se 3d, (c) S 2p, and (d) Zn 2p.

Figure 6 shows the X-ray photoelectron spectra of CdSe(S)@MPA QDs. The typical peaks of Cd $3d_{5/2}$ at 405.0 eV, Cd $3d_{3/2}$ at 411.6 eV, Se $3d_{5/2}$ at 53.8 eV, and S 2p at 161.6 eV confirm the existence of cadmium, selenium, and sulfur in the core QDs. When these QDs are treated with $Zn(OAc)_2$ in basic medium, a new peak originating from Zn $2p_{3/2}$ linked to oxygen atoms is observed at 1022.0 eV and confirms the successful capping of the CdSe(S) cores by the ZnO shell (Figure 7).

Photostability of CdSe(S)/ZnO QDs

Long-term stability of nanocrystal luminescence is one of the key problems for the application of QDs in light-emitting devices or bioimaging. Core/shell nanocrystals show significant enhancement in their photochemical stability relative to those of bare ones.

The photochemical instability of thioacid-capped CdSe QDs has already been studied. The photo-oxidation of the thioacid ligands in the presence of oxygen and light produces disulfides, which thus decomplex the nanocrystals and lead to aggregation.[34] As a result of this photo-oxidation, new surface defects are generated, the PL intensity decreases, and finally the QDs are bleached.[35–39] We compared the photostability of CdSe(S)/ZnO QDs with that of the parent CdSe(S) dots synthesized as in the literature.[14] PL spectra of aliquots of the two kinds of nanoparticles taken during continuous and intensive excitation between 300 and 350 nm with a Hg–Xe lamp (180 mW) and at ambient conditions are shown in Figure 8. As can be observed in Figure 8, the emission intensity of the MPA-capped CdSe(S) QDs drops rapidly and is reduced by ca. 60% after 8 min under continuous irradiation. In the meantime, the emission wavelength λ_{em} is bathochromically shifted by ca.

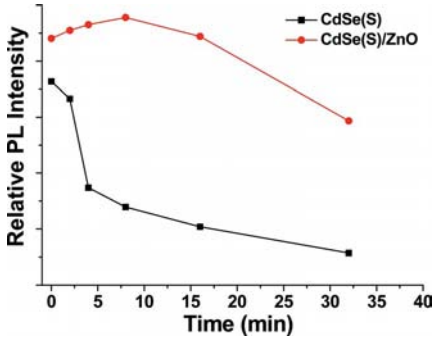

Figure 8. Photobleaching experiment of CdSe(S) and CdSe(S)/ZnO QDs in aqueous solution when irradiated between 300 and 350 nm with a Hg–Xe lamp.

 © 2011 Wiley-VCH Verlag GmbH & Co. KGaA, Weinheim

20 nm (from 512 to 525 nm, Figure 9b). The time evolution of the PL spectra observed in Figure 9b could be related to decomposition of the MPA ligand, which leads to free sulfide ions, which subsequently associate with Cd^{2+} to form a CdS shell around the CdSe(S) core. As observed with CdSe/CdS core/shell heterostructures,[40,41] because of the partial leakage of the exciton into the CdS shell, the growth of the shell results in a shift in the first exciton peak from 483 to 490 nm (Figure 9a) and a corresponding shift in the PL emission peak from 512 nm to 525 nm (Figure 9b). This decomposition of the MPA ligand reduces the stability of the QDs in water and leads to aggregation and precipitation of the nanocrystals.

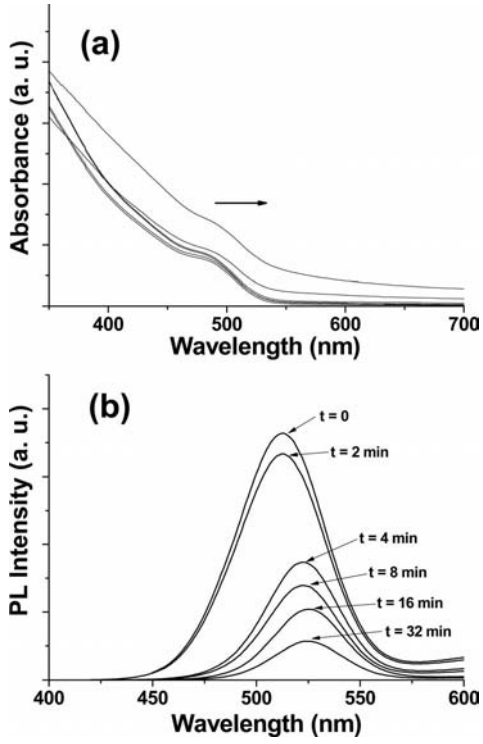

Figure 9. Time evolutions of (a) absorption spectra and (b) PL spectra of CdSe(S) QDs when irradiated between 300 and 350 nm with a Hg–Xe lamp.

In contrast, core/shell CdSe(S)/ZnO QDs have a much better performance under the same experimental conditions, as shown in Figure 10. A slight increase in emission intensity is observed during the first 8 min of irradiation, which indicates that these nanocrystals are very stable in aqueous solution (Figure 10b). A redshift in λ_{em} is only observed by further irradiating the sample (λ_{em} = 519 nm after 16 min, λ_{em} = 528 nm after 32 min). Finally, the luminescence intensity decreases significantly more slowly relative to that of the CdSe(S) cores.

To investigate the potential use in imaging applications, green-emitting core/shell CdSe(S)/ZnO QDs were used as staining probes of surface-attached microbial communities called biofilms. Biofilms are highly organized and structured microbial cells enmeshed in extracellular polymeric

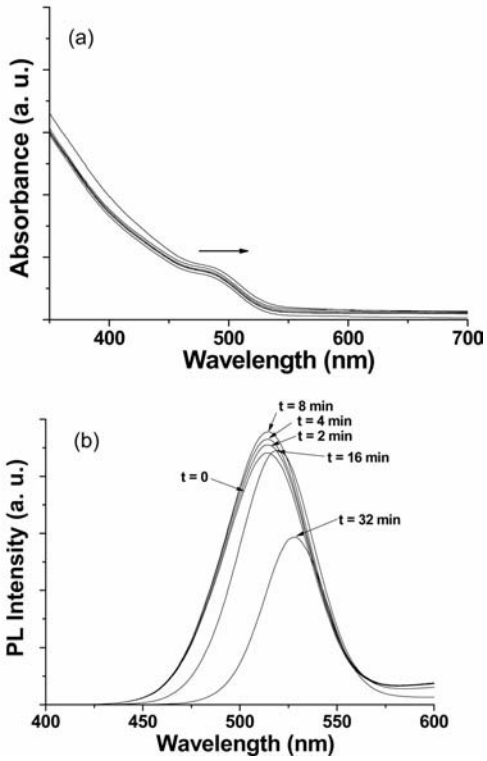

Figure 10. Time evolutions of (a) absorption spectra and (b) PL spectra of core/shell CdSe(S)/ZnO QDs when irradiated between 300 and 350 nm with a Hg–Xe lamp.

substances (EPS) of variable density and composition.[42] The EPS produced by microbial communities include a variety of biopolymers such as polysaccharides, proteins, nucleic acids, and amphiphilic compounds with different functionalities.[43] Because of their complexity, EPS are challenging to image. Staining of the EPS matrix could advance the current understanding of the development process and structural organization of biofilms, which would be essential for designing novel and effective antibiofilm therapies. For imaging experiments, biofilms of *Shewanella oneidensis* were grown for 48 h under the constant flow (200 μL/min) of a LML medium[44] supplemented with fumarate (0.5 mM) in flow cell systems that can be accommodated on a microscope set up. After the growth period, a 250 nM solution of CdSe(S)/ZnO QDs was injected by a syringe pump, and incubation was performed for 5 min. Unbound QDs were removed by washing the biofilm with fresh culture medium. Figure 11a and b show the transmission and the green channel confocal images, respectively, of a typical live, hydrated *S. oneidensis* biofilm at a focal plane 30 μm from the attachment substratum. As can be observed, MPA-capped CdSe(S)/ZnO QDs incorporate homogeneously into the biofilm and associate with the EPS matrix (higher-magnification photographs show that the QDs do not stain the bacterial cells). Vertical scanning of the sample shows that the QDs allow imaging of the biofilm over the full *z* range. Figure 11c shows in detail the fine three-dimensional structures of the labeled biofilm, includ-

 © 2011 Wiley-VCH Verlag GmbH & Co. KGaA, Weinheim

ing the mushroom-like protrusions and the aggregates of about 50-μm in thickness classically observed with such collections of surface-attached microorganisms.[45]

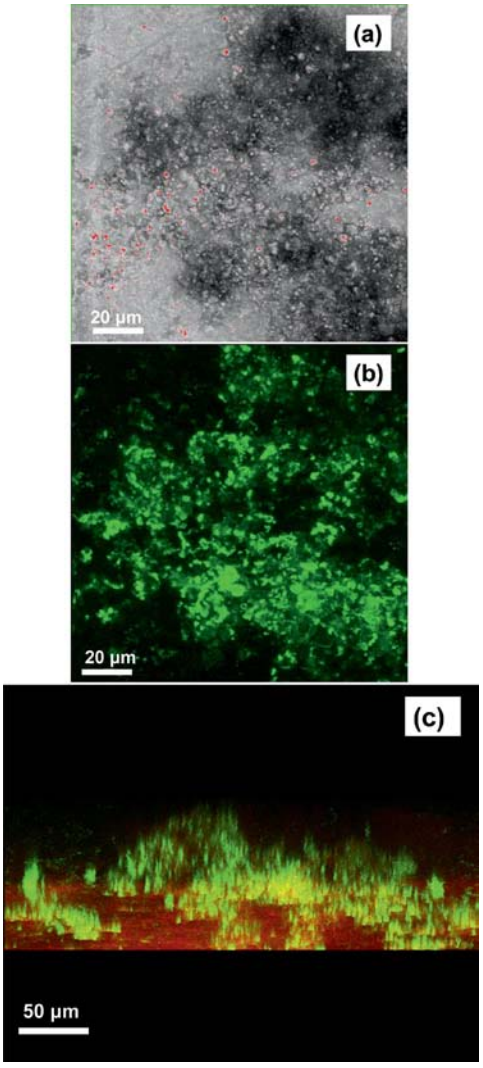

Figure 11. Confocal microscopy images of a *S. oneidensis* biofilm treated with CdSe(S)/ZnO QDs: (a) transmission image, (b) corresponding *XY* plane fluorescence image, and (c) image of the sum of *XY* planes. Confocal microscopy images were obtained with laser excitation at 405 nm.

Conclusions

The synthesis of a novel type of fluorescent semiconductor nanocrystals consisting of a alloyed CdSe(S) core and a ZnO outer shell has been developed. The synthetic methodology developed features easy handling and large-scale capability with mild reaction conditions and great reproducibility. The Zn/Cd ratio used for the preparation of core/shell CdSe(S)/ZnO QDs was studied to evaluate the influence of this variable on particle size and luminescence. At the optimum ratio (Zn/Cd = 0.4), a quantum yield of ca. 24% was achieved. The coating with the ZnO shell provides nanocrystals with more efficient and more stable luminescence than the starting CdSe(S) QDs. The potential of core/shell CdSe(S)/ZnO QDs for bioimaging applications was demonstrated by the labeling of *Schewanella oneidensis* bacterial biofilms.

Experimental Section

Chemicals: The chemicals used in the experiments included $CdCl_2 \cdot 2.5H_2O$ (99%), 3-mercaptopropionic acid (MPA, 99+%), sodium borohydride (96%), selenium powder (99.5%), $Zn(OAc)_2$ (99.99%), and isopropanol (*i*PrOH, HPLC grade). All chemicals were used without further purification. The water used in all experiments was deionized to a resistivity of 18.2 MΩ cm^{-1}.

Preparation of Water-Soluble CdSe(S) QDs: The preparation of NaHSe was performed according to Klayman et al.[46] with some modifications. $NaBH_4$ (76 mg, 2.009 mmol) was added to a small flask, cooled with ice, containing ultrapure water (1 mL) under a N_2 atmosphere. Selenium powder (79 mg, 1.004 mmol) was then added, and a small outlet was connected to the flask to discharge the hydrogen pressure generated by the reaction. After 3 h at 4 °C, the black selenium powder disappeared and a clear NaHSe solution was obtained. Under inert atmosphere, the solution was diluted with N_2-degassed water (20 mL). The concentration of the final NaHSe solution was 0.05 M.

The CdSe(S) QDs were prepared by reaction between $CdCl_2 \cdot 2.5H_2O$ and NaHSe in the presence of MPA as the stabilizing agent following the method described previously,[14] with some modifications. The molar ratio of Cd^{2+}/Se^{2-}/MPA was 8:1:8. Briefly, $CdCl_2 \cdot 2.5H_2O$ and MPA were dissolved in nitrogen-saturated ultrapure water (100 mL) ($[Cd^{2+}]$ = 10.9 mM), and the pH was adjusted to 11.2 with 1 M NaOH. The NaHSe solution was then added to the above precursor solution. The complex solution with a faint yellow color was put into a Teflon-lined stainless steel autoclave with a volume of 125 mL. The autoclave was maintained at 150 °C for 1 h and then cooled to room temperature.

Preparation of Core/Shell CdSe(S)/ZnO QDs: The Zn^{2+} injection solution (0.01 M) was prepared by dissolving $Zn(OAc)_2$ in aqueous solution. The molar ratio of Zn/Cd was 0.2 or 0.4. Briefly, the crude CdSe(S) QDs were first diluted to a concentration of 1.09×10^{-3} M, added to a three-necked flask, and heated in air at 100 °C. For a Zn/Cd ratio of 0.4:1, the $Zn(OAc)_2$ solution (2.2 mL) was first injected at a speed of 0.3 mL/min into the solution and further heated at reflux for 1 h. After that period, another portion of the $Zn(OAc)_2$ solution (2.2 mL) was injected, and the mixture was further heated for 1 h. The obtained CdSe(S)/ZnO QDs were precipitated by adding *i*PrOH and centrifuged at 4000 rpm. The QDs were dried in vacuo at room temperature and redissolved in water. Their concentration was estimated from the reported extinction coefficient per mol of particles (ε) by using the Beer–Lambert's law.[31]

Characterization: All the optical measurements were performed at room temperature (20 ± 2 °C) under ambient conditions. Absorption spectra were recorded on a Perkin–Elmer (Lambda 2, Courtaboeuf, France) UV/Vis spectrophotometer. Fluorescence spectra were recorded on a Fluorolog-3 spectrofluorimeter F222 (Jobin Yvon, Longjumeau, France) equipped with a thermostatted cell compartment (25 °C), by using a 450 W Xenon lamp. Quantum yield values were determined by the equation:

 © 2011 Wiley-VCH Verlag GmbH & Co. KGaA, Weinheim

$f_{sample} = (F_{sample}/F_{ref})(A_{ref}/A_{sample})(n_{sample}^2/n_{ref}^2)f_{ref}$

where F, A, and n are the measured fluorescence (area under the emission peak), the absorbance at the excitation wavelength, and the refractive index of the solvent, respectively. PL spectra were spectrally corrected, and the PL quantum yields were determined relative to Coumarin 153 in ethanol (f = 53%) by using the procedure recently developed by Grabolle et al.[47]

To determine the morphology and the diameters of the nanoparticles, the samples were analyzed ex situ by atomic force microscopy (AFM) and by transmission electron microscopy (TEM). AFM characterization was carried out by using a Digital Instruments Nanoscope III. AFM measurements were done by taping mode by using a Si_3N_4 tip with resonance frequency and spring constant of 100 kHz and 0.6 N m^{-1}, respectively, to provide surface topography. TEM images were taken by placing a drop of the particles in water onto a carbon film supported copper grid. Samples were studied by using a Philips CM20 instrument with LaB_6 cathode operating at 200 kV. Dynamic light scattering (DLS) was performed at room temperature with a Malvern zetasizer HsA instrument with a He–Ne laser (4×10^{-3} W) at a wavelength of 633 nm. The aqueous solutions of the QDs were filtered through Millipore membranes (0.2 μm pore size). The data were analyzed by the CONTIN method to obtain the hydrodynamic diameter (d_H) and the size distribution in each aqueous dispersion of nanoparticles. XPS measurements were performed at a residual pressure of 10^{-9} mbar, by using a KRATOS Axis Ultra electron energy analyzer operating with an Al-K_α monochromatic source. Powder (XRD) analyses were obtained by using Panalytical X'Pert Pro MPD diffractometer by using Cu-K_α radiation. The crystalline grain sizes were obtained by using the size broadening models built into Topas (Bruker) and by using the Fundamental Parameters approach.

Supporting Information (see footnote on the first page of this article): AFM images of the CdSe(S)/ZnO QDs and Rietveld refinement results of the powder XRD data of CdSe(S)/ZnO QDs are given.

Acknowledgments

This work was financially supported by the Agence Nationale pour la Recherche (ANR blanc 07, project DYNABIO). The authors thank Dr. Serge Corbel (LRGP, Nancy-University) and Marie-José Stebe (SRSMC, Nancy-University) for facilitating the photostability experiments and DLS measurements, respectively.

[1] Q. J. Sun, Y. A. Wang, L. S. Li, D. Y. Wang, T. Zhu, J. Xu, C. H. Yang, Y. F. Li, *Nat. Photonics* **2007**, *1*, 717–722.
[2] M. Bruchez Jr., M. Moronne, P. Gin, S. Weiss, A. P. Alivisatos, *Science* **1998**, *281*, 2013–2016.
[3] X. Michalet, F. F. Pinaud, L. A. Bentolila, J. M. Tsay, S. Doose, J. J. Li, G. Sundaresan, A. M. Wu, S. S. Gambhir, S. Weiss, *Science* **2005**, *307*, 538–544.
[4] V. L. Colvin, M. C. Schlamp, A. P. Alivisatos, *Nature* **1994**, *370*, 354–357.
[5] S. Coe, W. K. Woo, M. Bawendi, V. Bulovic, *Nature* **2002**, *420*, 800–803.
[6] A. L. Rogach, N. Gaponik, J. M. Lupton, C. Bertoni, D. E. Gallardo, S. Dunn, N. L. Pira, M. Paderi, P. Repetto, S. G. Romanov, C. O. Dwyer, C. M. S. Torres, A. Eychmuller, *Angew. Chem.* **2008**, *120*, 6638; *Angew. Chem. Int. Ed.* **2008**, *47*, 6538–6549.
[7] A. J. Nozik, *Phys. E* **2002**, *14*, 115–120.
[8] I. Gur, N. A. Fromer, M. L. Geier, A. P. Alivisatos, *Science* **2005**, *310*, 462–465.
[9] P. V. Kamat, *J. Phys. Chem. C* **2008**, *112*, 18737–18753.
[10] L. H. Qu, X. G. Peng, *J. Am. Chem. Soc.* **2002**, *124*, 2049–2055.
[11] A. L. Rogach, A. Kornowski, M. Gao, A. Eychmuller, H. Weller, *J. Phys. Chem. B* **1999**, *103*, 3065–3069.
[12] B. Nikoobakht, C. Burda, M. Braun, M. Hun, M. A. El-Sayed, *Photochem. Photobiol.* **2002**, *75*, 591–597.
[13] P. Zhong, Y. Yu, J. Wu, Y. Lai, B. Chen, Z. Long, C. Liang, *Talanta* **2006**, *70*, 902–906.
[14] F. Aldeek, L. Balan, J. Lambert, R. Schneider, *Nanotechnology* **2008**, *19*, 475401.
[15] J. V. Williams, N. A. Kotov, P. E. Savage, *Ind. Eng. Chem. Res.* **2009**, *48*, 4316–4321.
[16] F. Aldeek, L. Balan, G. Medjahdi, T. Roques-Carmes, J.-P. Malval, C. Mustin, J. Ghanbaja, R. Schneider, *J. Phys. Chem. C* **2009**, *113*, 19458–19467.
[17] J. Coulon, I. Thouvenin, F. Aldeek, L. Balan, R. Schneider, *J. Fluoresc.* **2010**, *20*, 591–597.
[18] L. P. Balet, S. A. Ivanov, A. Piryatinski, M. Achermann, V. Klimov, *Nano Lett.* **2004**, *4*, 1485–1488.
[19] H. Yang, P. H. Holloway, *Adv. Funct. Mater.* **2004**, *14*, 152–156.
[20] T. Mokari, U. Banin, *Chem. Mater.* **2003**, *15*, 3955–3960.
[21] E. A. Meulenkamp, *J. Phys. Chem. B* **1998**, *102*, 5566–5572.
[22] D. V. Talapin, A. L. Rogach, A. Kornowski, M. Haase, H. Weller, *Nano Lett.* **2001**, *1*, 207–211.
[23] M. A. Hines, P. Guyot-Sionnest, *J. Phys. Chem.* **1996**, *100*, 468–471.
[24] D. Pan, Q. Wang, S. Jiang, X. Ji, L. An, *J. Phys. Chem. C* **2007**, *111*, 5661–5666.
[25] J. Zhang, X. Zhang, J. Y. Zhang, *J. Phys. Chem. C* **2010**, *114*, 3904–3908.
[26] D. V. Talapin, I. Mekis, S. Götzinger, A. Kornowski, O. Benson, H. Weller, *J. Phys. Chem. B* **2004**, *108*, 18826–18831.
[27] S. J. Lim, B. Chon, T. Joo, S. K. Shin, *J. Phys. Chem. C* **2008**, *112*, 1744–1747.
[28] R. Xie, U. Kolb, J. Li, T. Basché, A. Mews, *J. Am. Chem. Soc.* **2005**, *127*, 7480–7488.
[29] A. L. Rogach, *Mater. Sci. Eng. B* **2000**, *69–70*, 435–440.
[30] A. L. Rogach, T. Franzl, T. A. Klar, J. Feldmann, N. Gaponik, V. Lesnyak, A. Shavel, A. Eychmüller, Y. P. Rakovich, J. F. Donegan, *J. Phys. Chem. C* **2007**, *111*, 14628–14637.
[31] W. W. Yu, L. Qu, W. Guo, X. Peng, *Chem. Mater.* **2003**, *15*, 2854–2860.
[32] B. O. Dabboussi, J. Rodriguez-Viejo, F. V. Mikulec, J. R. Heine, H. Mattoussi, R. Ober, K. F. Jensen, M. G. Bawendi, *J. Phys. Chem. B* **1997**, *101*, 9463–9475.
[33] Z. Deng, L. Cao, F. Tang, B. Zou, *J. Phys. Chem. B* **2005**, *109*, 16671–16675.
[34] J. Aldana, Y. A. Wang, X. Peng, *J. Am. Chem. Soc.* **2001**, *123*, 8844–8850.
[35] M. Nirmal, B. O. Dabboussi, M. G. Bawendi, J. J. Macklin, J. K. Trautman, T. D. Harris, L. E. Brus, *Nature* **1996**, *383*, 802–804.
[36] H. M. W. G. J. van Sark, L. T. Patrick, M. Frederix, D. J. Van den Heuvel, H. C. Gerritsen, *J. Phys. Chem. B* **2001**, *105*, 8281–8284.
[37] N. Myung, Y. Bae, A. J. Bard, *Nano Lett.* **2003**, *3*, 747–749.
[38] Y. Wang, Z. Y. Tang, M. A. Correa-Duarte, I. Pastariza-Santos, M. Giersig, N. A. Kotov, L. M. Liz-Marzan, *J. Phys. Chem. B* **2004**, *108*, 15461–15469.
[39] Y. Zhang, J. He, P.-N. Wang, J.-Y. Chen, Z.-J. Lu, D.-R. Lu, J. Guo, C.-C. Wang, W.-L. Yang, *J. Am. Chem. Soc.* **2006**, *128*, 13396–13401.
[40] G. Morello, M. Anni, P. D. Cozzoli, L. Manna, R. Cingolani, M. De Giorgi, *J. Phys. Chem. C* **2007**, *111*, 10541–10545.
[41] J. Zhang, X. Zhang, J. Y. Zhang, *J. Phys. Chem. C* **2010**, *114*, 3904–3908.

 © 2011 Wiley-VCH Verlag GmbH & Co. KGaA, Weinheim

[42] S. S. Branda, S. Vik, L. Friedman, R. Kolter, *Trends Microbiol.* **2005**, *13*, 20–26.
[43] M. Martin-Cereceda, B. Perez-Zu, S. Serrano, A. Guinea, *Water Sci. Technol.* **2002**, *46*, 199–206.
[44] T. K. Teal, D. P. Lies, B. J. Wold, D. K. Newman, *Appl. Environ. Microbiol.* **2006**, *72*, 7324–7330.
[45] D. de Beer, P. Stoodley, F. Roe, Z. Lewandowski, *Biotechnol. Bioeng.* **1994**, *43*, 1131–1138.
[46] D. L. Klayman, T. S. Griffin, *J. Am. Chem. Soc.* **1973**, *95*, 197–199.
[47] M. Grabolle, M. Spieles, V. Lesnyak, N. Gaponik, A. Eychmüller, U. Resch-Genger, *Anal. Chem.* **2009**, *81*, 6285–6294.

Received: July 21, 2010
Published Online: January 14, 2011

 © 2011 Wiley-VCH Verlag GmbH & Co. KGaA, Weinheim